

Direct Optical Imaging of Be Disks

Philippe Stee

*CNRS-UMR 6528
Département FRESNEL- Equipe GI2T
Observatoire de la Côte d'Azur
2130 route de l'Observatoire, Caussols,
06460 St Vallier de Thiey, France*

Abstract. Interferometry in the visible now provides milliarcsecond spatial resolution and thus can be used for studying the circumstellar environment of Be stars. In this review I will first introduce the two basic quantities that an interferometer can access: the modulus and the phase of the visibility. I will illustrate how these two quantities can be used to understand the physics of Be disks through recent results from the VLA, the MkII and the GI2T interferometers. I will insist on the importance and the potential of coupling high angular resolution with high spectral resolution to the study of Be disks. Since the possibility of direct optical imaging of Be disks will be limited due to complexity and time consumption, I will present the role models can play in interpreting high angular resolution observations when direct imaging become difficult. Finally I will draw up a list of challenging objectives for the next generation of synthetic arrays (GI2T/REGAIN, Keck, ST3, VLTI) which will bring new understanding of active hot stars physics.

1. Interferometry: a brief introduction

Observations with an imaging astronomical instrument can be described by the Image-Object relation given by a convolution product:

$$I(\rho) = O(\rho) \otimes T(\rho), \quad (1)$$

where $O(\rho)$ is the brightness distribution of the object across the sky and $T(\rho)$ is the point spread function of the instrument. Since the interferometric data reduction techniques are usually done through the analysis of the spectral density ($W(f)$) in the Fourier space (see Mourard et al. 1994 and Berio et al. 1999), we can use the Fourier transform of eqn. (1):

$$\tilde{I}(\vec{f}) = \tilde{O}(\vec{f}) \cdot \tilde{T}(\vec{f}), \quad (2)$$

where the convolution product of eqn.(1) is now a simple product between $\tilde{O}(\vec{f})$ and $\tilde{T}(\vec{f})$, which are respectively the Fourier transform of O and T . $\tilde{T}(\vec{f})$ is called the optical transfer function.

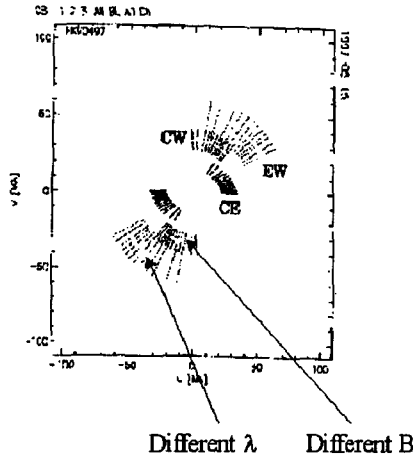


Figure 1. NPOI (u,v) plane coverage for the Mizar binary observations. (Benson, with permission)

The relation with the spectral density $W(f)$, where the estimation of the fringe contrast is done, is given by:

$$W(\vec{f}) = |\tilde{I}(\vec{f})|^2 = |\tilde{O}(\vec{f})|^2 |\tilde{T}(\vec{f})|^2 \tag{3}$$

Thus it is completely similar to describe the object through its brightness distribution or through its Fourier transform. The vector \vec{f} in eqn. (2) and (3) is the spatial frequency and is given by:

$$\vec{f} = \frac{\vec{B}}{\lambda}, \tag{4}$$

where λ is the observing wavelength and \vec{B} is the interferometer baseline projected onto the skyplane. In order to obtain information on the object brightness distribution, not only in one direction, one has to change the modulus of the projected baseline \vec{B} but also its orientation. This technique, called the (u,v) plane coverage can be done thanks to the Earth's rotation a few hours before and after the transit of the star. This is the "super-synthesis effect" or it can be done by moving two or more telescopes in two dimensions. From eqn. (3) it is also possible to increase the (u,v) plane coverage by changing the wavelength λ but with the hypothesis that the object brightness distribution is constant within the considered wavelength's range. An example of a (u,v) plane coverage is shown in Fig. 1 from actual observations of NPOI interferometer (Benson et al. 1997).

The information that is needed for astrophysical studies is the fringe visibility (V) which is a complex quantity, i.e. $V = |V| \exp^{i\phi}$. In the quasi-monochromatic case, the modulus of the complex degree of coherence of the source is equal to the modulus of the normalized spatial Fourier transform of the source's brightness. Thus the visibility modulus can be written as:

$$|V| = \frac{|\tilde{O}(\vec{f})|}{|\tilde{O}(0)|} \quad (5)$$

In the (X- λ) mode, used specially on the GI2T, the fringes are dispersed by a grating spectrograph in the horizontal direction and it is thus possible to combine high angular resolution (~ 1 mas) and medium spectral resolution (~ 1 Å).

For an unresolved source the visibility is constant and equal to one, whereas it drops to zero when one starts to resolve the star. For an idealized apparent uniform disk, the visibility curve follows a $|2\frac{J_1(z)}{z}|$ function with a first zero for the resolving baseline B_r (in meters) given by:

$$B_r \sim 250 \frac{\lambda}{\phi_{ud}}, \quad (6)$$

where ϕ_{ud} is the stellar diameter (in mas) and λ is the wavelength in microns.

2. First result using a large (u,v) plane coverage: the Be star ψ Per observed with the VLA radio interferometer

These observations were done with the VLA radio interferometer by Dougherty & Taylor 1992. The synthesized beam full width at half maximum (FWHM) of the VLA interferometer was 176×144 mas. The high projected rotational velocity of ψ Per (300 km s^{-1}) indicates that the rotation axis of the star lies closely to the plane of the sky. The detection of centimeter wavelength radio emission due to free-free emission demonstrates that the gas extends to very large radii. The major axis found at 15 GHz is more than 34 times its diameter at visible wavelengths. Assuming that their data represents the diameter of the optically thick emitting region, they found a linear size to the radio emission of $3700 R_{\odot}$ at a distance of 155 pc. The angular size of the source allowed them to determine a lower limit to the brightness temperature of 870 K which is also a lower limit to the kinetic temperature of the electrons. The results are summarized in Table 1, and the reconstructed map is shown on Fig. 2. Note that the new distance for ψ Per determined from Hipparcos (215 ± 34 pc) leads to a linear size to the radio emission larger than $5000 R_{\odot}$.

Table 1. ψ Per observed with the VLA radio interferometer

Wavelength	15 GHz
Major axis	111 ± 16 mas
Position angle	$158^{\circ} \pm 10^{\circ}$
Minor axis	Unresolved < 68 mas

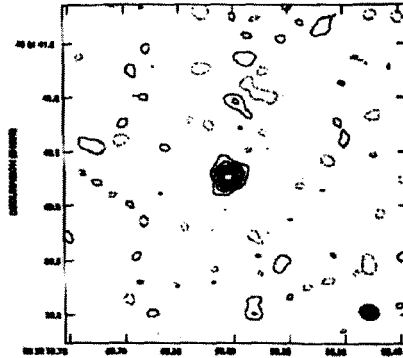


Figure 2. ψ Per observed with the VLA radio interferometer. The FWHM of the beam (black dot) at the lower right corner is 176 x 144 mas (Dougherty, with permission)

3. Results from the Mk III interferometer

The Mk III interferometer was a Michelson interferometer with two 2.5 cm siderostats on a single north-south baseline between 3.0 and 31.5 m located at Mount Wilson (U.S.A) (see Shao et al. 1988 for a detailed description of the instrument). The capability of this instrument was exploited to cover a large (u,v) plane by using the “super-synthesis” effect and definitively proved that Be stars envelopes are not spherical. For instance, Quirrenbach et al. (1993), found that γ Cas envelope is elongated to the East from 20° with respect to the North-South direction. These authors also found that if the envelope is symmetric with respect to the rotation axis the inclination angle of this axis must be at least 42° . These results confirm the usual picture for the origin of the linear polarization by electron scattering in a flattened envelope (see Fig. 3).

Quirrenbach et al. (1994) have also reconstructed an intensity map, using a maximum of entropy algorithm, of the Be star ζ Tau, showing for the first time how flattened a Be star’s envelope can be. The disk of ζ Tau is certainly seen edge-on and they were able to derive an inclination angle of at least 73° , assuming an axially symmetric rotation axis (see Fig. 3).

Quirrenbach et al. (1997) obtained constraints on the geometry of the circumstellar envelopes of seven Be stars using optical interferometric observations in the $H\alpha$ emission line from the Mk III interferometer and polarimetric data from the PBO spectropolarimeter at the University of Wisconsin. Their results are summarized in Table 2 (note that the photometric diameters are not interferometric measurements but are taken from Barnes-Evans relation). The envelope diameters are smaller than 5 mas for the 7 Be stars. Among these 7 stars, 4 were not circularly symmetric and showed evidence of elongation. The result (3.47 mas) for γ Cas agrees well with the diameter in the N-S direction of 3.25 ± 0.4 mas measured by Thom et al. 1986 with the I2T interferometer.

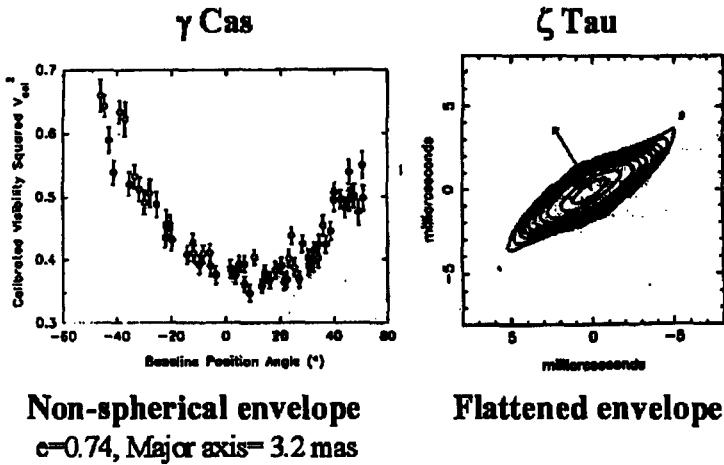


Figure 3. γ Cas and ζ Tau observed with the Mk III interferometer (Quirrenbach, with permission)

The position angles of the major axis of the elongation were in agreement with the disk orientation determined from polarization data and also with the result from radio observations for ψ Per. It means that there is no misalignment between the larger scale envelope from the radio observation ($\sim 100R_*$), the intermediate scale from H α emission ($\sim 10 R_*$), and the inner regions where the polarization is produced.

An important result comes from the agreement shown in Table 3 between the position angles of the circumstellar disks derived from interferometric measurements and those from polarimetric data. For all cases the polarization angle is perpendicular to the major axis, which rules out envelope that are both op-

Table 2. Photospheric and disk diameters from the MkIII interferometer (From Quirrenbach et al. 1997)

Star	V	photosphere (mas)	envelope (mas)	env/photo	W(H α) Å
γ Cas	2.47	0.56	3.47	6.2	20.1
ϕ Per	4.07	0.39	2.67	6.8	53.8
ψ Per	4.23	0.35	3.26	9.4	38.0
η Tau	2.87	0.71	2.65	3.8	6.0
48 Per	4.04	0.34	2.77	8.0	19.7
ζ Tau	3.00	0.39	4.53	11.6	22.0
β CMi	2.85	0.74	2.65	3.6	5.4

Table 3. Comparison of position angles from polarimetric and interferometric observations (from Quirrenbach et al. 1997).

Star	Disk Position Angle (deg.)	
	Interferometry	Polarimetry
γ Cas	$19^\circ \pm 2$	$20.6^\circ \pm 0.4$
ϕ Per	$-62^\circ \pm 5$	$-65.6^\circ \pm 0.3$
ψ Per	$-33^\circ \pm 11$	$-44.8^\circ \pm 0.7$
η Tau	(19)	...
48 Per	(68)	...
ζ Tau	$-58^\circ \pm 4$	$-57.9^\circ \pm 0.1$
β CMi

tically and geometrically thick since they produce polarization parallel to the plane of the disk.

Nevertheless, we must be cautious with the diameters of the circumstellar envelopes given in table 2 since the Mk III interferometer observations were done using a narrow filter (10 Å) centred on the H α line. In fact, most of the 7 stars exhibited H α line profile widths larger than 10 Å (see last column in Table 2). This is an important point since line flux is lost not only in the wings of the profile but through spatial filtering. Thus, there is potential confusion due to “cross-talk” of flux produced from iso-velocity regions and from other regions which emit line flux at wavelengths outside the bandpass limits of the H α filter.

4. Results from the GI2T interferometer

The GI2T/REGAIN interferometer is a Michelson interferometer with two 1.5m telescopes on a single north-south baseline between 12.0 and 65.0 m located at Caussols, France (see Mourard et al. 1994a, 1994b and 1998) for a detailed description of the instrument). This instrument uses the dispersed fringes technique ($X-\lambda$ mode) which permits studies of the circumstellar environment of Be stars with an angular resolution of ~ 1 mas in the visible and a spectral resolution of ~ 1 Å. Thus, it is possible to study the size of an emitting region at different wavelengths and also within a given spectral line.

Stee et al. (1998) reported spectrally resolved observations of γ Cas in the He I $\lambda 6678$ and H β emission lines. They concluded that the H β emitting region must be < 8.5 stellar radius and ≈ 2.3 stellar radii in He I $\lambda 6678$. This is, for He I $\lambda 6678$, smaller than the nearby continuum extent. These results confirmed the basic parameters for γ Cas obtained by Stee et al., 1995 (see Table 4). A summary of GI2T’s observations of γ Cas is shown in Figure 4.

In the previous sections only the modulus of the visibility was exploited. With the GI2T interferometer it is also possible to follow the phase of the visibility as a function of wavelength and/or time. The phase of the visibility is related to the source photocenter position onto the skyplane (see Fig. 5). For

Table 4. Parameters and results for γ Cassiopeiae (From Stee 1996)

Parameters	
Spectral type	B0.5IVe
Effective temperature	25000 K
Mass	16 M_{\odot}
Radius	10 R_{\odot}
Stellar angular diameter	0.45 mas
Luminosity	$3.5 \cdot 10^4 L_{\odot}$
$V \sin i$	230 km s^{-1}
Inclination angle i	45°
Results	
Polar terminal velocity	2016 km s^{-1}
Polar mass flux	$1.7 \cdot 10^{-9} M_{\odot} \text{ yr}^{-1} \text{ sr}^{-1}$
Equatorial terminal velocity	200 km s^{-1}
Equatorial mass flux	$5.1 \cdot 10^{-8} M_{\odot} \text{ yr}^{-1} \text{ sr}^{-1}$
Mass loss rate	$3.2 \cdot 10^{-7} M_{\odot} \text{ yr}^{-1}$
$H\alpha$ major axis	17 stellar radii
$H\alpha$ oblateness	0.72
$H\alpha$ extension	4 mas
He I $\lambda 6678$ extension	0.51 mas
$H\beta$ extension	<1.91 mas
Continuum extension at 650 nm	0.78 mas
Continuum extension at 480 nm	0.63 mas
Mass of the disk	$6.4 \cdot 10^{-8} M_{\odot}$

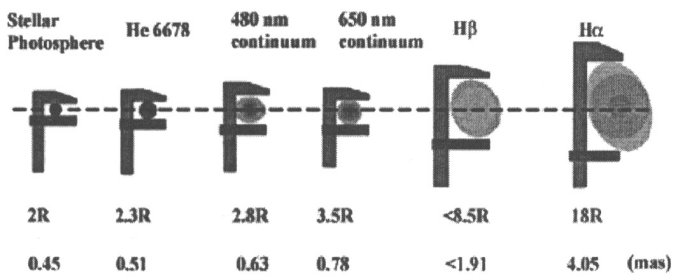


Figure 4. GI2T observations of γ Cas at different wavelengths

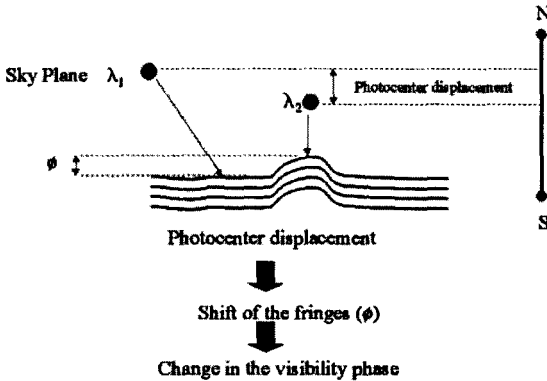


Figure 5. Phase of the visibility as a function of wavelength

instance if one takes the continuum emission as a reference source (which is not really the best reference since the envelope can contribute up to 20% of the total continuum emission, see Stee et al. 1994), one can nevertheless follow the photocenter displacement as a function of the doppler shift across the $H\alpha$ line profile at different epochs.

4.1. “One-armed” oscillations in the Be Shell star ζ Tau and in the Be star γ Cas

Observing the Be shell star ζ Tau in October 1993, Vakili et al. (1998) found that a high density pattern was observable at a radial velocity of about $+130 \text{ km s}^{-1}$ and has a north-south projection position of 0.7 mas to the south of the continuum source (i.e at $3.6 R_*$). By October 1994, this density pattern had rotated progradely and its signature occurred at a radial velocity of -70 km s^{-1} . It was by then located at 0.5 mas to the north of the continuum source which corresponds to $2.6 R_*$. These observations are the first detection of an axisymmetric envelope around a Be star and are interpreted as a direct evidence for a prograde rotation of a one-armed equatorial disk (see Fig. 6 for a schematic representation of the long term variability of ζ Tau’s $H\alpha$ emission).

After ζ Tau, γ Cas is the second Be star for which interferometric observations show direct evidence for a prograde one-armed oscillations of its equatorial disk (see Fig. 7).

This prograde precession agrees with the Okazaki’s model (Okazaki 1997) of the one-armed ($m=1$) oscillation confined by the radiative effect. In their paper on γ Cas, Berio et al. 1999 have investigated the possibility of such an oscillation occurring within the equatorial regions of a latitude-dependent radiative wind model developed by Stee & Araújo (1994). In this model, the star is distorted due to its high rotation. The centrifugal force makes the effective gravity and the brightness temperature decrease from pole to equator. Thus the corresponding radiative force will depend on the stellar latitude. Finally, the star has a highly ionized fast wind in the polar regions and a slow wind of low ionization, with a higher density near the equator. In the inner ($\leq 10 R_*$), cool, dense equatorial regions the kinematics is dominated by the Keplerian rotation,

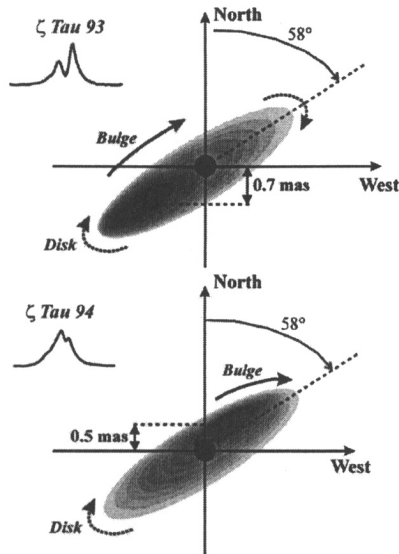
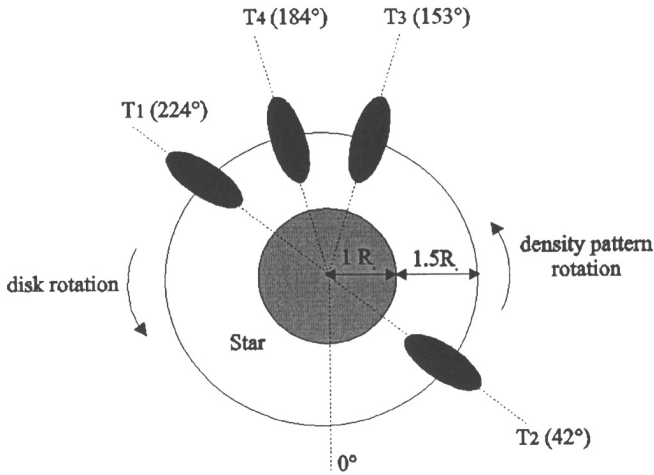


Figure 6. Schematic representation of ζ Tau $H\alpha$ long term variability (Vakili, with permission)

the radiative wind is due to optically thin lines where the one-armed oscillations develop. The global period of the oscillation remains about 7 years, which is consistent with the mean value found by Hirata & Hubert-Delplace (1981) from spectroscopic observations.

4.2. Interferometric observations of β Lyr international multitechnique campaign in 1994

Studies of interacting Be binaries have also benefited from high angular resolution observations. A paper by Harmanec et al. (1996) confirms the spatial orientation of the projection of the vector of the orbital angular momentum on the sky ($\theta = 160^\circ$ from the North). Moreover, interferometric, spectroscopic, photometric, and polarimetric data confirm that the bulk of the $H\alpha$ and HeI 6678 emission seems to originate from jets perpendicular to the orbital plane. These jets are associated with the more massive (primary) component of the binary. They may originate from a “hot-spot” in the disk where the gas stream is flowing through the Roche lobe of the second component (B6-8 II) toward the primary. It seems that some contribution to the emission may also come from an intermediate region between the two stars. This result agrees well with the analysis of UV line polarization.



High density pattern in γ Cas equatorial disk

Figure 7. Schematic representation of γ Cas one-armed oscillations, confined in its equatorial plane at $1.5 R_*$. (Berio, with permission)

5. Differential speckle interferometry of γ Cas

This technique is the same as that described for long baseline interferometry but in this case a single telescope is used and the speckle positions are followed in the image plane as a function of wavelength. The results of Sanchez (1996) indicate that the envelope of γ Cas is neither spherical nor axisymmetric.

6. Velocity law in the disk of γ Cas

In the study of the rotational component of the wind in the envelope of γ Cas Stee 1996 found that constant and solid body rotation laws can be rejected. Nevertheless, following the variation of the photocenter displacement into the sky plane they were not able to distinguish between a momentum conservation ($\beta = 1.0$), a Keplerian ($\beta = 0.5$) and a $\beta = 0.25$ circular velocity law.

7. Models for the interpretation of future high angular resolution observations

In order to obtain direct images, one has to control the phase of the fringes between different triplets of telescopes. This technique called "phase closure" has been already tested with the COAST and NPOI interferometers (Cambridge, MRAO and Anderson Mesa, Lowell Observatory), and have produced nice images of the binary star Capella in the near IR (Baldwin et al. 1996) and of Mizar A at visible wavelengths (Benson et al. 1997). Nevertheless, even with future interferometric networks, due to the complexity and time consumption, direct images of Be stars will be limited to only a few objects. Moreover, even if one

obtains nice images of Be stars, one will need models to interpret data and to be more quantitative (see for instance the astrophysical quantities presented in Table 4). These models must be able to reproduce visibility curves and intensity maps (with more classical observables, i.e. spectroscopic and photometric ones) since a few visibility points at “strategic” spatial frequencies can put very strong constraints. Such models have been developed and exploited successfully with the GI2T interferometer (see for instance the SIMECA code by Stee et al. 1994, 1995) and other theoretical models such as Wind Compressed Disk (WCD) (Bjorkman & Cassinelli 1993) or “one-armed” oscillations (Okazaki 1991) have to produce high angular resolution observables.

8. Challenging objectives

For the next generation of synthetic arrays (GI2T/REGAIN, Keck, ST3, VLTI), I have drawn up a short list of challenging objectives, starting from the easiest to the most difficult:

1. measure the photospheric diameters: needs baselines up to 200m,
2. Study the connection between the disk and the photosphere: needs high precision visibility measurements,
3. study the rotation in the disk: needs high spectral resolution and phase measurements,
4. measure the size of one-armed structure in the disk and follow its rotation. Is it connected to the star?;, needs spectral and spatial resolution,
5. study details on the photosphere, i.e NRP versus magnetism: needs large baselines, spectral resolution, and a polarimetric device as well,
6. detect stellar ejections: needs spectral, spatial and time resolution,
7. Make direct images at different wavelngts in narrow bands: needs spectral, spatial, time resolution and phase closure.

References

- Armstrong et. al. 1998, ApJ 496, 550
Baldwin et al. 1996, A&A, 306, L13
Benson, J.A., Hutter, D.J., Elias II, M. et al. 1997 AJ 114, No 3, p 1221
Berio, Ph, Stee, Ph., Vakili, F. et al. 1999, A&A, 354, 203
Berio, Ph., Mourard, D., Bonneau, D. et al. 1999, JOSA A, Vol 16, No 4, p 872
Bjorkman, J. E., & Cassinelli, J. P. 1993, ApJ 409, 429
Dougherty, S. M. & Taylor, A. R. 1992, Nature, 359, 808
Harmanec, P., Morand, F., Bonneau et al. 1996, A&A, 312, 879.
Hirata, R. & Hubert-Delpace, A.-M., 1981, in:G.E.V.O.N., Sterken C. (eds.)
Workshop on Pulsating B Stars. Nice Observatory, p 217

- Mourard D., Tallon-bosc I., Blazit A., Bonneau D., Merlin G., Morand F., Vakili F., Labeyrie A. 1994a, *A&A*, 283, 705
- Mourard D., Tallon-bosc I., Rigal F., Vakili F., Bonneau D., Morand F., Stee Ph. 1994b, *A&A*, 288, 675
- Mourard, D., Thureau, N., Antonelli, P., et al. 1998, *SPIE Conference on Astronomical Interferometry*, 3350, p 517
- Okazaki, A. T. 1991, *PASJ*, 43, 75
- Okazaki, A. T. 1997, *A&A*, 318, 548
- Quirrenbach A., Hummel C. A., Buscher D. F. et al. 1993, *ApJ* 416, L25
- Quirrenbach A., Buscher D. F., Mozurkewich D. et al. 1994, *A&A*, 283, L13
- Quirrenbach A., Bjorkman K. S., Bjorkman J. E. et al. 1997, *ApJ* 479, 477
- Sanchez, L., Petrov, R. G., Vasyuk, V. et al. 1996, *Science With the VLT interferometer*, *Proceedings of the ESO Workshop*, Garching, Germany, ed. F. Paresce, Springer, p 393
- Shao, M., Colavita, M. M., Hines, B. E., et al. 1988, *A&A* 193, 357
- Stee, Ph., & Araújo, F.X., 1994, *A&A*, 292, 221.
- Stee, Ph., Araújo, F. X., Vakili, F., Mourard, D., Arnold, L., Bonneau, D., Morand, F. and Tallon-Bosc, I. 1995, *A&A*, 301, 219.
- Stee, Ph. 1996, *A&A*, 311, 945
- Stee, Ph., Vakili, F., Bonneau, D. et al. 1998, *A&A*, 332, 268
- Thom, C., Granès, P. and Vakili, F. 1986, *A&A*, 165, L13
- Vakili F., Mourard D., Stee Ph., et al. 1998, *A&A*, 335, 261.

Discussion

P. Najarro: In your model fits to $H\alpha$, there seems to be some discrepancies on the wings. Have you tried to use the HeI 6678 line which forms deeper to constrain the velocity field? It seems to me that only with $H\alpha$ you still have too many free parameters.

Ph. Stee: There is not really a large difference in the wings of the $H\alpha$ line profile between the observed and the computed one. The discrepancy is more in the small “bump” that is present in our computed profile close to the central $H\alpha$ wavelength (in the blue part of the line) but which is not observed. We have not used the HeI 6678 line to constrain the velocity field and I agree that it may help. We have not used only the $H\alpha$ line profile to adjust our free parameters (which are not so many!). We have also used the energy distribution, the visibility curves in the continuum, the whole $H\alpha$ line and also 13 narrow channels across this line. This model is the first “physical” model that agrees well with the photometry, the $H\alpha$ line and high angular spectrally resolved data.

J. Bjorkman: You have ruled out solid body rotation for the disk of γ Cas. Can you distinguish between Keplerian and angular momentum conserving rotation laws?

Ph. Stee: No, we cannot distinguish between Keplerian and angular momentum conserving rotation laws. We hope, with the new REGAIN beam combiner we will be able to address this issue in the coming months.